

PTEase: Objective Airway Examination for Pulmonary Telemedicine using Commodity Smartphones

Xiangyu Yin, Kai Huang, Erick Forno, Wei Chen, Heng Huang and Wei Gao University of Pittsburgh USA

ABSTRACT

Remote monitoring and evaluation of pulmonary diseases via telemedicine are important to disease diagnosis and management, but current telemedicine solutions have limited capability of objectively examining the airway's internal physiological conditions that are crucial to pulmonary disease evaluation. Existing solutions based on smartphone sensing are also limited to externally monitoring breath rates, respiratory events, or lung function. In this paper, we present PTEase, a new system design that addresses these limitations and uses commodity smartphones to examine the airway's internal physiological conditions. PTEase uses active acoustic sensing to measure the internal changes of lower airway caliber, and then leverages machine learning to analyze the sensory data for pulmonary disease evaluation. We implemented PTEase as a smartphone app, and verified its measurement error in labcontrolled settings as <10%. Clinical studies further showed that PTEase reaches 75% accuracy on disease prediction and 11%-15% errors in estimating lung function indices. Given that such accuracy is comparable with that in clinical practice using spirometry, PTEase can be reliably used as an assistive telemedicine tool for disease evaluation and monitoring.

CCS CONCEPTS

 \bullet Human-centered computing \rightarrow Ubiquitous and mobile computing;

KEYWORDS

Pulmonary Telemedicine, Airway Examination, Acoustic Sensing, Smartphone, Multi-Task Learning

ACM Reference Format:

Xiangyu Yin, Kai Huang, Erick Forno, Wei Chen, Heng Huang and Wei Gao. 2023. PTEase: Objective Airway Examination for Pulmonary Telemedicine using Commodity Smartphones. In *ACM International Conference on Mobile Systems, Applications, and Services (MobiSys '23), June 18–22, 2023, Helsinki, Finland.* ACM, New York, NY, USA, 14 pages. https://doi.org/10. 1145/3581791.3596854

1 INTRODUCTION

Pulmonary diseases, such as asthma and chronic obstructive pulmonary disease (COPD), were the fourth cause of death in the US before the COVID-19 pandemic [33] and are hence a major public

Permission to make digital or hard copies of all or part of this work for personal or classroom use is granted without fee provided that copies are not made or distributed for profit or commercial advantage and that copies bear this notice and the full citation on the first page. Copyrights for components of this work owned by others than the author(s) must be honored. Abstracting with credit is permitted. To copy otherwise, or republish, to post on servers or to redistribute to lists, requires prior specific permission and/or a fee. Request permissions from permissions@acm.org.

MobiSys '23, June 18-22, 2023, Helsinki, Finland

© 2023 Copyright held by the owner/author(s). Publication rights licensed to ACM. ACM ISBN 979-8-4007-0110-8/23/06...\$15.00 https://doi.org/10.1145/3581791.3596854

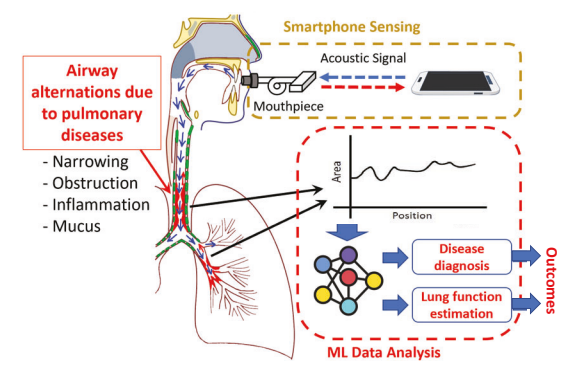


Figure 1: Overview of PTEase design

health issue [3]. Diagnosis and management of these diseases are often based on subjective symptom reports by patients, but patients usually fail to recognize early small symptoms or slow decline in lung function with chronic diseases, especially when being out of clinic [4, 6, 18]. This poor perception leads to acute exacerbations resulting in emergency department visits and hospitalizations [9, 39]. Evaluating pulmonary diseases remotely but objectively via telemedicine, hence, is crucial to disease management, both acutely and in the long term.

Telemedicine has enormous potential to improve pulmonary disease evaluation and symptom control [11, 15]. These advantages are particularly important in the COVID-19 pandemic, with pulmonary patients unable or unwilling to attend clinic visits or use shared equipment. However, current telemedicine has mostly been limited to video calls that still rely on subjective symptom self-report [31], with limited or no capability of objectively examining airway conditions.

To address this deficiency, current sensing techniques either attach force sensors [24], ultrasound sensors [43, 50] or inductive bands [8, 46] onto the human body, or use expensive systems such as infrared cameras [2, 29], depth cameras [59] or RF systems [25, 30, 37, 60]. However, their requirement for extra hardware results in limited usability in long-term telemedicine. Using smartphones for sensing can address this limitation, but most existing solutions are limited to monitoring breath rates or respiratory events (e.g., apnea) [35, 36], which are not directly related to pulmonary disease evaluation. Other techniques measure lung function externally by passively overhearing the breathing sounds [21, 28, 34] or actively measuring chest mobility [51], but they cannot examine the airway's alternations of internal physiological conditions, such as airway obstruction and restriction caused by inflammation and mucus hypersecretion [14, 17], which are crucial to pulmonary disease evaluation.

In this paper, we aim to bridge the above gap between clinical needs and current sensing techniques, by presenting *PTEase*, a new system design that transforms a commodity smartphone into a

pulmonary telemedicine examination device. As shown in Figure 1, PTEase uses active acoustic sensing to measure the internal changes of lower airway caliber that reflect alternations of airway conditions, and then leverages machine learning (ML) to analyze the airway measurements for pulmonary disease evaluation. PTEase's sensing approach transmits acoustic signals from smartphone speakers into the airway via a 3D-printed disposable passage, and analyzes the received signal reflected from airway lumen by extending the traditional acoustic reflection technique (ART), to calculate the cross-sectional area (CSA) of each airway segment. PTEase's data analysis approach uses a multi-task learning model, which provides both disease prediction and estimation of lung function.

The major challenge in ensuring accurate airway measurement is that the reflected acoustic signal from the airway could be reflected again in the passage and cause extra echoes. These echoes are difficult to be removed and the smartphone's received acoustic signal is hence a mixture of the airway's reflected signal and the passage's echoes. PTEase addresses this challenge using three steps of calibrations with low operational costs. We first collect the directly transmitted signal from smartphone speaker to microphone without any reflection, and then use this signal to derive the transfer function between the airway's reflected signal and echoes, from which the echoes can be unmixed from the received signal.

In practical telemedicine settings, the accuracy of calibrations could be affected by various system and human factors. To address the impact of system factors, PTEase develops a quantitative metric to evaluate the quality of each airway measurement, and uses such quality evaluation to decide the best calibration data being used. We also designed an ergonomic mouthpiece and the corresponding examination protocols to minimize the impact of human factors, such as unintentional tongue movements and breathing sounds.

Analyzing airway measurements for pulmonary disease evaluation, on the other hand, could be affected by the high variability in airway measurements, which weakens the correlation between these measurements and disease symptoms and make it difficult for ML models to correctly learn such correlation. A common approach to reducing the learning difficulty is to incorporate the corresponding domain knowledge into ML model design. When training the ML model in PTEase, we first use self-supervised learning to extract distinctive features from airway measurements. Then, we use the users' spirometry data from their health records¹ as the domain knowledge about users' lung function to supervise the training and enhance the training feedback.

To our best knowledge, PTEase is the first system that uses commodity smartphones to directly measure the human airway's internal physiological conditions, compared to existing works that are mostly limited to indirect measurements of heartbeat [48], breathing rate [21, 62] or lung function [28, 51] from external observations. PTEase hence provides an important telemedicine tool to assist clinical decisions in pulmonary disease management. Key characteristics of PTEase are as follows:

- PTEase is accurate. When being evaluated in lab-controlled settings, its measurement error is always lower than 10%.
- PTEase is effortless and can be conveniently used out of clinic whenever needed. Being different from traditional PFT

- methods such as spirometry, PTEase does not require any forced maneuvers or difficult protocols, and can be used during normal breaths.
- PTEase is adaptive. It can precisely remove the impacts from various system and human factors, and can hence be widely applied to different smartphone models and environmental settings.
- PTEase is *lightweight*. It does not require any extra computing hardware, and only consumes <20% of the smartphone's battery life with 1-hour usage.

By collaborating with clinical pulmonologists and biostatisticians at the Children's Hospital of Pittsburgh, we conducted a clinical study of 12 months over 182 patients with a wide variety of different ages, genders, races, body conditions, and diseases. With the hospital's IRB approval², 495 valid airway measurements are collected. The results of our clinical study are as follows:

- PTEase achieves an average accuracy of 75% when predicting the patient's disease status. This accuracy is comparable to that of spirometry for diagnosing asthma [49] and CF [26].
- PTEase restrains the error of estimating lung function indices within 15%, which is also comparable to current spirometers being used in clinic [44].
- PTEase achieves high accuracy of airway measurements over different patient subgroups, divided by age, gender, and disease. It is hence widely applicable to a large population of patients.

2 BACKGROUND AND MOTIVATION

In this section, we first provide background knowledge about pulmonary diseases and the current clinical methods being used in pulmonary disease evaluation. Then, we motivate our design of PTEase by highlighting the limitations of these existing methods and the difficulty of directly replicating these methods on commodity smartphones.







Figure 2: Airway conditions in pulmonary diseases. A) normal; B) asthma; C) cystic fibrosis

2.1 Pathology of Pulmonary Diseases

As shown in Figure 2, alterations of the airway's internal physiological conditions are a fundamental part of many pulmonary diseases, and can be reflected by the corresponding changes in airway caliber. In asthma, airway inflammation causes swelling and acute bronchoconstriction, leading to narrowing that causes symptoms and exacerbations. Severe asthma can lead to airway remodeling and more permanent narrowing. COPD is partly caused by progressive inflammatory damage to airways and alveoli (the tiny air sacs in the lungs that perform gas exchange), leading to airway obstruction and decreased lung recoil, both affecting lung function. In cystic fibrosis (CF), abnormally thick and sticky mucus clogs the airways

¹In clinical practice, spirometry data is essential for pulmonary disease management, and are hence always available in pulmonary patients' electronic health records (EHR) [5, 22].

 $^{^2 \}rm University$ of Pittsburgh IRB approval No. STUDY20040181-01.

and allows bacteria to grow, leading to chronic inflammation and recurrent infections. As a result, in PTEase we measure the changes in airway caliber as the indicator of pulmonary disease conditions.

2.2 Pulmonary Function Tests

Current pulmonary disease evaluations are mostly based on pulmonary function tests (PFTs) [12]. Spirometry, as the most commonly used PFT, uses forced breathing efforts to measure breath volumes and velocities under maximum exhalation, and produce lung function indices including 1) forced vital capacity (FVC), 2) forced expiratory volume in 1 second (FEV1), and 3) the ratio of FEV1 to FVC (FEV1/FVC). Since lung function greatly varies among individuals, clinicians categorize subjects into subgroups according to their demographics (e.g., age, gender, race, etc.), and convert the raw values of spirometry indices into percentiles in each subgroup [42]. Typically, significantly low percentiles (<70%) are the key indicators of pulmonary diseases.

However, forced maneuvers in spirometry make it difficult to be used in telemedicine without professional coaching [16, 20], and spirometers in-home use are known to be highly inaccurate [38, 41]. In PTEase, we instead aim to provide effortless airway examination methods that do not require any forced maneuvers or difficult protocols.

2.3 Acoustic Methods for Airway Examination

Some techniques have been developed to replace the forced maneuvers in spirometry, by actively transmitting acoustic waves to probe the internal conditions of the airway. Forced oscillation technique (FOT) [40] and impulse oscillometry (IOS) [13] use pressure waves to measure the airway's overall resistance and impedance, but cannot provide detailed information about the conditions of different airway segments.

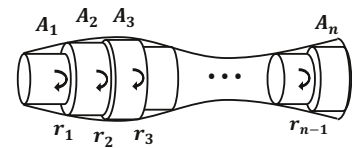


Figure 3: Calculating airway CSA in an ART system

The acoustic reflection technique (ART) [23] addresses this limitation by measuring the cross-sectional areas (CSA) at different airway positions. As shown in Figure 3, the transmitted acoustic signal pulses are assumed to propagate in the airway as 1-D plane waves, which will only be reflected on the boundary between airway segments with different CSAs. Then, the CSA of the k-th airway segment (A_k) is iteratively calculated using the Ware-Aki (WA) algorithm [55] as $A_{k+1}/A_k = (1-r_k)/(1+r_k)$, where r_k indicates the ratio between reflected and incident signals at the boundary. In practice, the WA algorithm first calculates the airway's impulse response (IR) from deconvolution between the transmitted and received signals. Then, given the Z-transform of impulse response (h(t)) as $H(z) = \sum_{k=1}^{\infty} H_k z^{-k}$, r_k can be calculated from H_1, H_2, \cdots, H_k .

It is, however, challenging to replicate the ART system design to commodity smartphones. As shown in Figure 4(a), an ART system uses a connecting tube to direct the acoustic signal into the airway, but the reflected signal from airway could be reflected again by the sound source and create infinite echoes in the tube, referred as

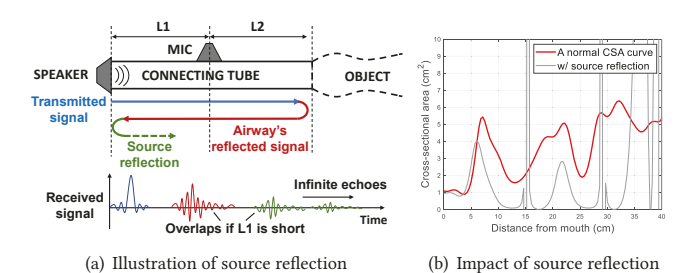


Figure 4: Source reflection in airway measurements

source reflection. These echoes overlap with the airway's reflected signal and create extra measurement errors, as shown in Figure 4(b). A traditional ART system addresses this issue by placing the microphone on the tube wall to be far away from the speaker (>50cm), to separate the airway's reflected signal and echoes in time. This solution, however, is infeasible on smartphones where the placements of bottom speaker and microphone are very close and fixed. This difficulty motivates us to design new measurement protocols and signal processing algorithms for accurate CSA measurements on smartphones.

3 OVERVIEW

As shown in Figure 5, the 3D-printed disposable passage in PTEase consists of a smartphone adaptor, a connecting tube, and a mouth-piece. To use PTEase, the user connects the passage to the phone, places the mouthpiece in the mouth, handholds the smartphone, and breaths normally through the passage for a few seconds. No forced maneuvers (e.g., deep breath and forceful exhalation), difficult protocols, or extra computing hardware are needed. The PTEase app on the smartphone transmits a series of acoustic pulses, each of which lasts 2ms, into the airway. It is hence able to obtain hundreds of airway measurements within each second, eliminating the impact of random system noise.

With the received acoustic signal, PTEase uses the WA algorithm described in Section 2.3 to calculate the airway's impulse response and converts it to airway CSA measurement. A prerequisite is that the acoustic signal propagation in the airway is a 1-D plane wave, and this assumption holds if the signal wavelength is smaller than two times of airway diameter: higher-order wave reflections will only be non-negligible when the transmitted signal's frequency is higher than the cut-off frequency [19, 56]. Since the diameters of most human airway structures, including trachea, pharynx, and larynx, are smaller than 3cm [7, 52], the maximum frequency of the transmitted signal is 5.7 kHz, which has a satisfactory gain on most smartphone models. Although this frequency falls in the audible bands, signal propagation is confined within the passage with >35dB attenuation. Hence, using PTEase has negligible impact on users' health.

On the other hand, acoustic signal propagation in the airway could also be affected by the non-rigidity of airway lumen: the axial variation in airway impedance due to such non-rigidity may produce extra signal reflection, which can be falsely interpreted as CSA changes and result in over-estimation of airway CSA [23]. However, since such over-estimation bias equally applies to all system use cases, it can be considered as a system offset and can hence be effectively removed by calculating the relative CSA difference between different subject groups in practical disease evaluation.

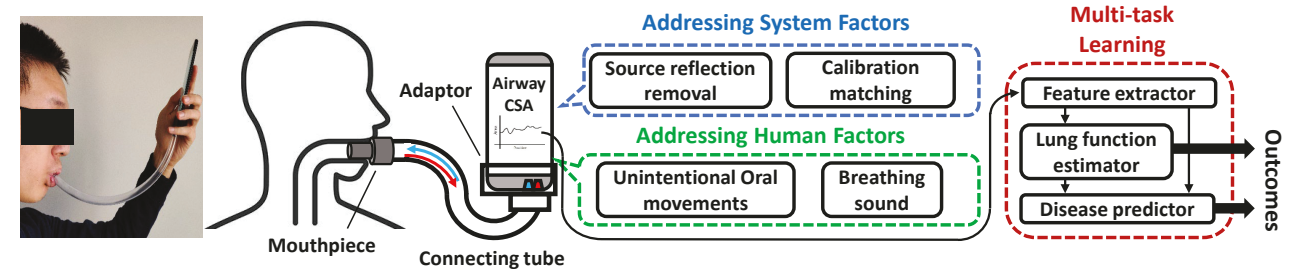


Figure 5: PTEase System Overview

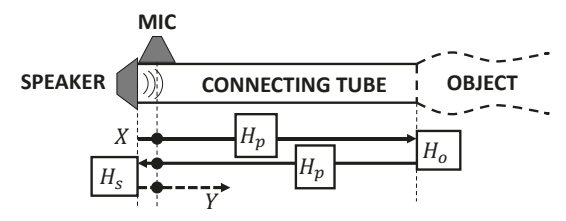


Figure 6: Analytical modeling of source reflection

To achieve objective and precise disease evaluation, our design of PTEase aims to address the impacts of possible system and human factors that may affect the accuracy of airway measurement, and also aims to minimize the user's discomfort during airway measurements. Afterwards, these measurements are used as input to a multi-task ML model that evaluates pulmonary disease conditions, including the probability of disease and lung function indices.

3.1 Addressing System Factors

To address the impact of source reflection described in Section 2.3, we start with the analytical model of acoustic signal reflection and propagation in the connecting tube. When the reflected signal is a linear transformation of the incident signal without frequency shift, both the airway's reflection and source reflection are considered as linear time-invariant (LTI) systems with different transfer functions. For an input signal x(t) and the corresponding LTI system output y(t), in the complex frequency domain of Laplace transform, we have Y(s) = H(s)X(s) where H(s) is the system's transfer function. As shown in Figure 6, we denote the transfer function of source reflection, airway's reflection, and signal propagation in the tube as $H_s(s)$, $H_o(s)$ and $H_p(s)$, respectively. Smartphone's received signal Y(s) can be written as a function of the transmitted signal Y(s):

$$\begin{split} Y(s) = & X(s) + H_p^2(s) H_o(s) X(s) \\ & + H_p^2(s) H_o(s) H_s(s) X(s) + H_p^4(s) H_o^2(s) H_s(s) X(s) + \cdots, \end{split}$$

where the high-order terms indicate the infinite echoes caused by source reflection. This can be further generalized as the following infinite geometric sequence:

$$Y(s) = \left[X(s) + H_p^2(s)H_o(s)X(s)\right] \cdot \sum_{n=0}^{\infty} \left[H_p^2(s)H_o(s)H_s(s)\right]^n$$

$$= X(s) \frac{1 + H_p^2(s)H_o(s)}{1 - H_p^2(s)H_o(s)H_s(s)}.$$
(1)

To calculate the impulse response $h_o(t) = \mathcal{L}^{-1}\{H_o(s)\}$ of airway, we need to estimate $X(s), H_p(s)$ and $H_s(s)$, all of which only relate to the measurement system (smartphone and passage) rather than the airway. Hence, our approach to these estimations is three steps of

calibrations that obtain different characteristics of the measurement system. Details of these calibrations are in Section 4.1.

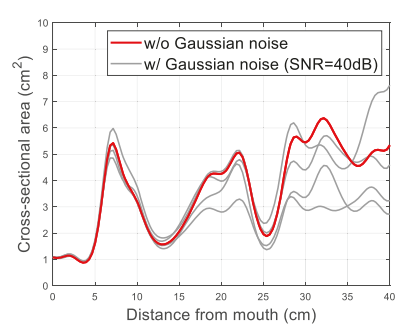


Figure 7: Accumulation of errors in CSA measurements due to different system placements

In practical telemedicine, the users need to do calibrations and airway measurements themselves, by assembling the system components (smartphone, adaptor, connecting tube, and mouthpiece) in different ways. However, these assemblies may cause slightly different placements of system components: the adaptor may be sleeved to different positions, and the connecting tube may be slightly tilted or bent. Such different placements could lead to mismatching between calibration and use setups, introducing measurement errors. In particular, since the WA algorithm iteratively calculates the CSA of airway segments, measurement error will accumulate in calculations and be amplified in lower airway segments. To verify this, we add white Gaussian noise with 40dB SNR to a received signal collected from an adult healthy male and the results in Figure 7 show that the measurement error in upper airway segments (distance from mouth is <25cm) is within 20%, but could be amplified to 100% or higher in lower airway segments.

Addressing this problem requires measuring the tiny difference between different system placements, which is difficult. Instead, our solution is to improve the calibration by applying random noise to the original calibration data and constructing a calibration data library. In each measurement, we apply all calibration data in the library to the received signal and select the result with the highest quality. Details of such selection are in Section 4.2.

3.2 Addressing Human Factors

When PTEase is used in telemedicine by different subject groups who differ in physiological conditions and behavior patterns, various human factors may affect airway measurements and we will need to minimize their impacts.

Oral movements. First, the outlet of the mouthpiece in PTEase should be ideally aligned to the subject's throat, so that acoustic

signals can be smoothly transmitted into the airway. However, the mouthpiece may be misaligned due to the user's unintentional oral movements, including irregular movements of the tongue and expansion of the oral cavity during exhalation, and hence incur extra measurement errors as shown in Figure 8. Our solution is to develop a new ergonomic mouthpiece design that minimizes these oral movements and maximizes comfort. Details of such mouthpiece design are in Section 5.1.

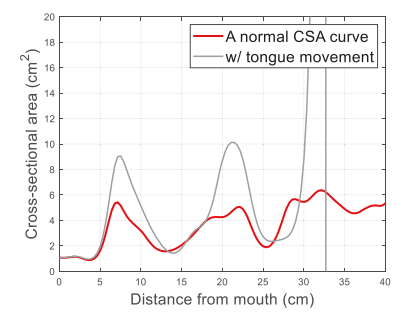


Figure 8: Impact of unintentional tongue movements collected from an adult healthy male using PTEase

Breathing sound. When the users breathe through PTEase's passage, the breathing airflow goes through the smartphone's microphone and may hence produce audible sounds that affect airway measurement accuracy as shown in Figure 9. To minimize its impact, we measure the received signal strength between the transmitted signal pulses at runtime, to detect such breathing sounds and issue a warning to the user via PTEase smartphone app for slower breaths. No deep breath is required, though. Any remaining breathing sound will be removed by a digital Wiener filter and details of such removal are in Section 5.2.

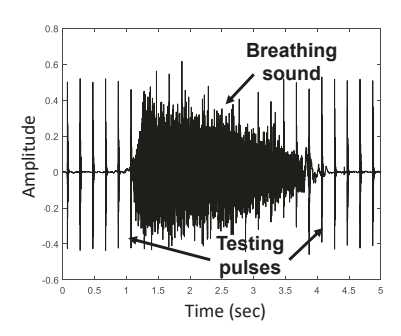


Figure 9: Loud breathing sound in a received signal

3.3 Pulmonary Disease Evaluation

With airway CSA measurements, PTEase uses a multi-task learning model to provide both disease prediction and lung function estimation. The major challenge, as shown in Figure 10, is the high variability of airway measurements, even on the same subject in one PTEase use. Such variability is caused by both system noise and physiological airway movements during measurements. It weakens the correlation between airway measurements and disease symptoms, and hence makes it difficult for ML models to make predictions from any single airway measurement.

Instead, our solution is to first construct high-dimensional input data from multiple CSA measurements, to eliminate the variability.

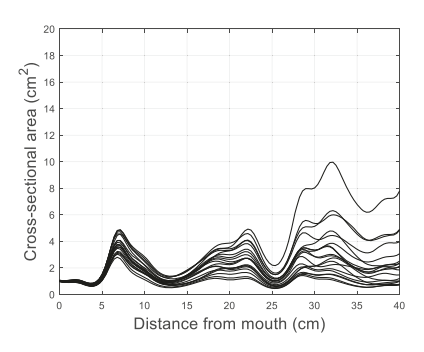


Figure 10: Multiple airway measurements collected from the same adult healthy male using PTEase

Then, we first use self-supervised learning to reduce the learning difficulty by extracting distinctive features, and then incorporate domain knowledge provided by the user's spirometry data into our NN model training. Details of such multi-task learning are in Section 6.

SYSTEM CALIBRATIONS TO ENSURE ACCURATE MEASUREMENTS

In this section, we provide technical details about the system calibrations in PTEase that ensure accurate airway measurements by eliminating the impact of various system factors.

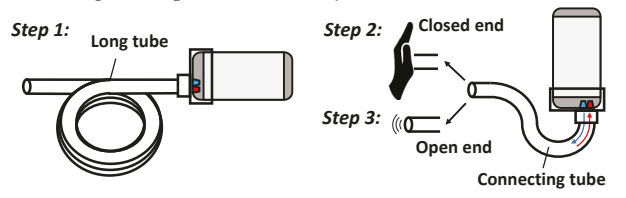


Figure 11: Three steps of calibration to remove the impact of source reflection

4.1 Three-Step Calibrations

As shown in Figure 11, we remove the impact of source reflection using three steps of calibrations that estimate X(s), $H_{D}(s)$ and $H_{S}(s)$. In the first step, we replace the connecting tube with a sufficiently long tube (e.g., >5m). The smartphone's microphone will then receive no reflection signal but only the speaker's transmitted signal, ensuring precise estimations of X(s). Note that since X(s) only relates to characteristics of smartphone speaker and microphone, this step only needs to be done once on each smartphone device.

In the next two steps, we use the normal connecting tube without the mouthpiece, block the tube outlet by hand (Step 2) and then release it (Step 3). They give a fully positive reflection (i.e., $H_o(s) =$ 1) and a fully negative reflection (i.e., $H_o(s) = -1$) of incident signal, respectively. Denote the received signal in these two steps as $Y_1(s)$ and $Y_2(s)$, we have:

$$Y_1(s) = X(s) \frac{1 + H_p(s)^2}{1 - H_p^2(s)H_s(s)}, Y_2(s) = X(s) \frac{1 - H_p(s)^2}{1 + H_p^2(s)H_s(s)}.$$
 (2)

Therefore, we can get

$$H_p(s)^2 = \frac{[Y_1(s) + Y_2(s)]X(s) - 2Y_1(s)Y_2(s)}{[Y_1(s) - Y_2(s)]X(s)},$$

$$H_p^2(s)H_s(s) = \frac{Y_1(s) + Y_2(s) - 2X(s)}{Y_1(s) - Y_2(s)},$$
(4)

$$H_p^2(s)H_s(s) = \frac{Y_1(s) + Y_2(s) - 2X(s)}{Y_1(s) - Y_2(s)},\tag{4}$$

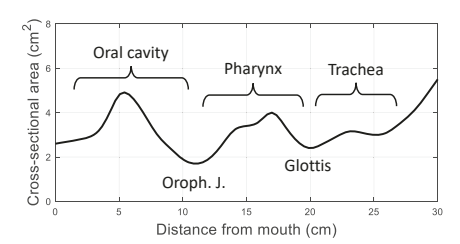


Figure 12: The reference airway CSA curve

from where we can compute $H_p(s)$ and $H_s(s)$ from X(s), $Y_1(s)$ and $Y_2(s)$.

This procedure of three-step calibration is fully automated, and the only operation that needs to be manually done by the user is to plug/unplug the long and standard connecting tubes to/from the adapter. According to our observations in our clinical study described in Section 9, such calibration procedure can be easily operated by children in low ages within one minute. Furthermore, the first calibration step only needs to be done once for each smartphone device, and can hence operated by us before distributing the smartphones to users. Step 2 and 3 of calibrations are only needed when the user replaces the smartphone adapter, which could usually last several uses. As a result, this calibration procedure, as a whole, brings a negligible amount of extra efforts to users.

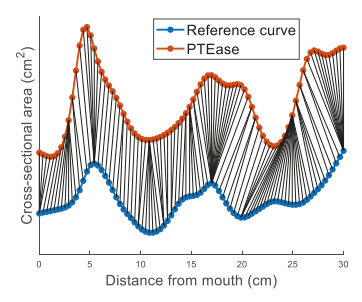


Figure 13: Using DTW to align airway measurements

4.2 Selecting the Best Calibration Data

When we apply all data in the calibration data library to the received signal, we obtain different airway measurements and select one with the highest quality. We evaluate the quality of a measurement by comparing it with the reference airway CSA curve used in clinical ART [27]. As shown in Figure 12, the reference curve indicates airway physiological structures, including oral cavity, oropharyngeal junction (Oroph. J.), pharynx, glottis, and trachea.

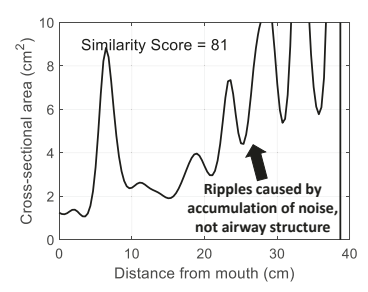
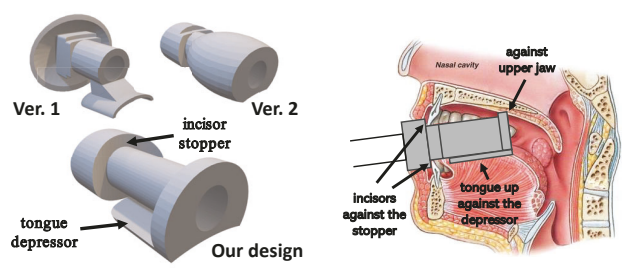


Figure 14: Low-quality curves with high scores

However, simple distance-based similarity metrics cannot be adopted, because of the heterogeneity of airway lengths in different



(a) Different designs of mouthpieces

(b) Usage of PTEase mouthpieces

Figure 15: Mouthpiece design

user groups. Instead, we use dynamic time warping (DTW) [32] to stretch different airway measurements and align them to the same scale. As shown in Figure 13, DTW calculates the best match between two given sequences with the minimum mean squared error (MSE), and a similarity score between 0 and 100 can be calculated from the MSE to indicate the measurement quality.

Solely using such similarity scores to evaluate measurement quality may not be always reliable in practice. Due to the DTW's stretching mechanism, some measurements, as shown in Figure 14, may have high quality scores but still contain large errors. To address this limitation and ensure reliability, we further use a neural network (NN) classifier to identify unacceptable airway measurements. The training data is a small amount of CSA measurements from different individuals and we manually label these data's quality as acceptable or unacceptable. Then, we only accept an airway measurement for disease evaluation if it has high quality score and passes the NN classifier's test. The threshold of high quality score is determined by examining a subset derived from the whole dataset, to make sure all selected CSA measurements follow the characteristics illustrated in Figure 12.

5 REMOVING THE IMPACTS OF HUMAN FACTORS

In this section, we provide technical details about how PTEase removes the impact of various human factors on the accuracy of airway measurement.

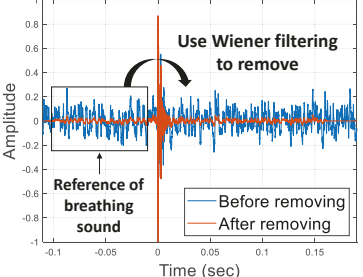


Figure 16: Breathing sound removal

5.1 Mouthpiece Design

Mouthpieces in PTEase are expected to 1) fully seal the oral cavity to prevent acoustic signal leakage, 2) prevent possible mouthpiece mobility in the mouth, and 3) minimize unintentional tongue movements. Some simple designs, such as Ver. 1 and Ver. 2 shown in Figure 15(a), fail to accomplish these objectives. The Ver. 1 design uses a large oval lip stopper that causes discomfort, and uses a small tongue depressor that cannot avoid tongue movements. The Ver. 2

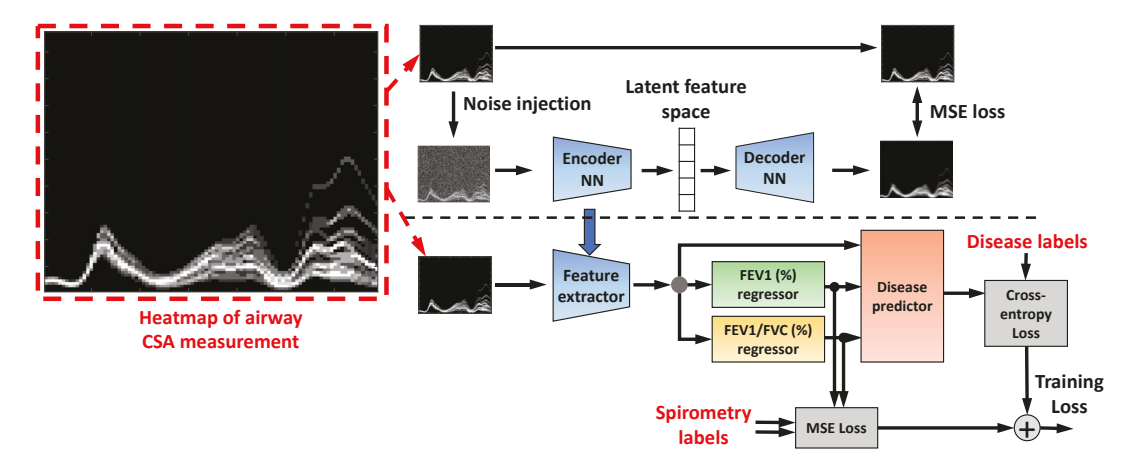


Figure 17: Machine learning for pulmonary disease evaluation

design uses an ellipsoid body for tongue depression, but cannot be comfortably placed in the mouth.

Instead, we develop a new ergonomic mouthpiece design that fits the physiological structure of human oral cavity. As shown in Figure 15(a), our design first includes an incisor stopper on the inlet to fix its orientation when the user bites. Then, a tongue depressor at the bottom ensures that the mouthpiece outlet is always oriented toward the throat, when the user is instructed to press the tongue up against the depressor as shown in Figure 15(b). In this way, both ends of the mouthpiece are fixed in the oral cavity, hence minimizing its possible mobility during airway measurements. To further minimize the user's discomfort, we designed mouthpieces in different scales (100%/90%/75%/50%) to fit patients of different ages. Our ergonomic mouthpiece design has been validated in our clinical study to produce minor discomfort.

5.2 Addressing Breathing Sounds

Acoustic sensing in PTEase works best with slow breaths, but does not require any deep breath or forced breath efforts. If the user breathes too fast, loud breathing sounds may introduce extra measurement errors. Our solution is to first locate the breathing sound in the received signal, by comparing the strength of the received signal with the transmitted signal pulses. Whenever breathing sound is detected between two transmitted pulses, we use a digital Wiener filter to remove the breathing sound. As shown in Figure 16, we first collect a short segment of breathing sound before the transmitted pulse, as the reference input to the Wiener filter. Then, by assuming that the signal characteristics of the breathing sound remain unchanged over time, the Wiener filter uses this reference to remove the breathing sound after the transmitted pulse, based on minimum mean square error (MMSE) estimation. Further, this Wiener filter also helps mitigate the impact of undesired system noise, ensuring a sufficiently high SNR for precise disease evaluation.

6 MULTI-TASK LEARNING FOR PULMONARY DISEASE EVALUATION

As shown in Figure 17, to reduce the learning difficulty caused by high variability of airway measurements, we convert multiple airway CSA measurements of a subject into a heatmap as highdimensional input data. Our multi-task learning model then consists of a feature extractor, two regressors that estimate lung function indices, and a predictor that gives disease predictions.

6.1 Constructing High-Dimensional Input

To construct the heatmap as high-dimensional input data, we consider the multiple CSA measurements at each airway position as a distribution of discrete samples, and conduct non-parameterized estimation to convert these samples into a continuous function that depicts airway dimensions. The heatmap is then produced by concatenating such estimated functions across the entire airway. The heatmaps are then used as one-channel images for the ML model input.

6.2 Training the Feature Extractor

We use a symmetric encoder-decoder architecture to train a convolutional auto-encoder as a prerequisite step, and then use the trained encoder as the feature extractor in later training of the multi-task learning model. The key challenge of training the feature extractor is overfitting due to the limited amount of available input data from human subjects. To address this challenge, we leverage self-supervised learning to blur the input heatmaps with random Gaussian noise, and set the learning objective as restoring the original input heatmap, by using the mean-square error (MSE) between the restored and original heatmaps as the loss function. In this way, the encoder automatically learns to the representative features that are sufficiently informative for the decoder to restore the original heatmap.

6.3 Training the Lung Function Estimators & Disease Predictor

To ensure informative training feedback, our basic rationale is that PTEase's airway measurement and traditional spirometry provide two different modalities for measuring pulmonary disease conditions and complement each other. Since spirometry is widely regarded as the current gold standard in pulmonology, spirometry measurements are regularly documented and always available in patients' health records. Spirometry measurement results, hence, could serve as pre-known domain knowledge to supervise the training of our ML model and provide extra training feedback to ensure training convergence. All the spirometry data used in training were

collected in patients' stable conditions rather than their acute exacerbation. Since most pulmonary diseases are chronic and patients' lung functions remain stable in the long term when no acute exacerbation happens, we believe that spirometry data in stable conditions could provide more generic and objective information about the patients' lung functions.

As shown in Figure 17, the extracted features are used as the input to two regressors that predict the user's FEV1 and FEV1/FVC percentile, the two most representative lung function indices, respectively. The regressors' outputs are supervised by the MSE loss from spirometry data, and are also used as the input to the disease predictor that estimates the corresponding pulmonary disease probability. The physician's clinical diagnosis of disease condition, which are extracted from the users' health records and jointly made from the users' symptoms, lung functions and bronchodilator tests [45], are used as the disease labels to compute cross-entropy loss and supervise the disease predictor's output. The MSE loss and cross-entropy loss, then, are aggregated as the training loss.

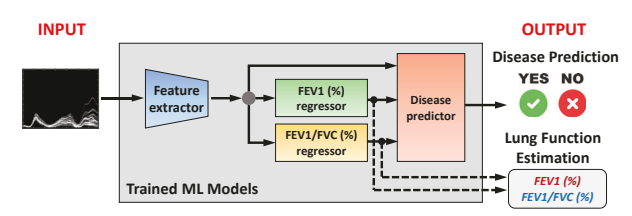


Figure 18: Inference stage of the ML model

In particular, note that our approach only uses the patients' spirometry data to supervise the ML model training. As shown in Figure 18, after the model training completes, we will only use the airway CSA measurements as the input to the trained disease predictor and regressors for disease evaluation at runtime. As a result, PTEase does not require the user to conduct spirometry tests or provide spirometry measurements when using the telemedicine system for disease evaluation, and such disease evaluation consists of two outputs: 1) disease prediction (e.g., yes/no for asthma/CF) and 2) estimated lung function indices (e.g., FEV1 and FEV1/FVC).

7 IMPLEMENTATION

As shown in Figure 19, we implemented PTEase as an Android app, which senses the airway, analyzes the received signal, and uploads data to a remote server³. Before each airway measurement, text instructions will be displayed on the screen. To conduct a test, the user only needs to click once on the START button, and the entire test procedure afterwards will be fully automated. During the test, the app will instruct the user to inhale or exhale multiple times with a countdown timer. After each measurement, the app shows the measurement results and warns the user if loud breathing sounds were produced. We also made multiple smartphone adaptor designs for different smartphone models and mouthpieces in different sizes for different user groups.

We implemented our algorithms of acoustic signal processing in C and used Android Native Development Kit (NDK) to compile the source codes into a native Android library, which is then being

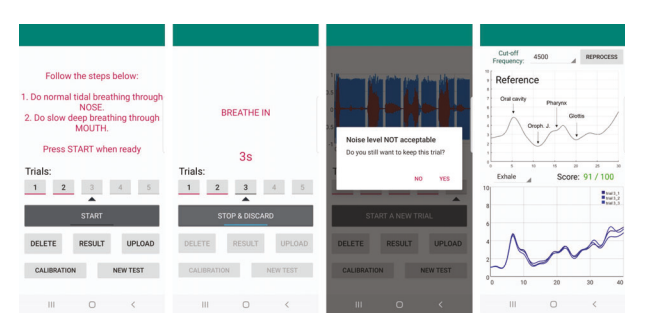


Figure 19: PTEase smartphone app UI

invoked by Android's Java Native Interface (JNI) at runtime. After a user completes the whole test, the airway CSA measurements are uploaded to the ML model deployed on a cloud server. In our implementation of the multi-task learning model, each module is a 3-layer feedforward network, and the autoencoder contains a $100 \times 48 \times 48$ CNN encoder and a $48 \times 48 \times 100$ CNN decoder. The ML model is trained using Adam optimizer, with a step size of 0.001 and a batch size of 32.

8 PERFORMANCE EVALUATION

In this section, we evaluate the performance of PTEase's airway measurement in lab-controlled settings, with different measurement targets. First, we concatenate soft PVC tubes with different pre-known CSAs, as shown in Figure 20(b), and use PTEase to measure these CSAs. Second, we use anonymized human subjects' chest CT scans provided by the Children's Hospital of Pittsburgh to make 3D-printed models of the lower airway and upper airway segments, and then connect them with plastic tubes, as shown in Figure 20(b), to be the measurement target. The lower airway model is further printed in three different sizes, i.e., the 100%, 90%, and 80% scale of the airway diameter, to emulate different lower airway conditions. Third, we also recruit healthy student volunteers to conduct human tests. Each volunteer is instructed to conduct three complete PTEase measurements, and the results are evaluated using the quality metrics described in Section 4.2.





(a) Concatenated plastic tube

(b) 3D-printed human airway model

Figure 20: Measurement targets in lab-controlled settings

8.1 Measurement Accuracy

We first examine the measurement accuracy of PTEase on concatenated plastic tubes, by running PTEase on a Samsung Galaxy S8 smartphone. Experimental settings with different tube CSAs and the corresponding measurement results are shown in Figure 21. PTEase can achieve high measurement accuracy, and the mean absolute percentage error (MAPE) is $8.13 \pm 2.25\%$ among different combinations of tube CSAs.

³The source codes of our acoustic sensing algorithms, ML models and smartphone app can be found at: https://github.com/ericyxy98/PTEase. The source code repository also contains a demo video to help better understand PTEase's operations, especially its calibration procedure and smartphone app operations.

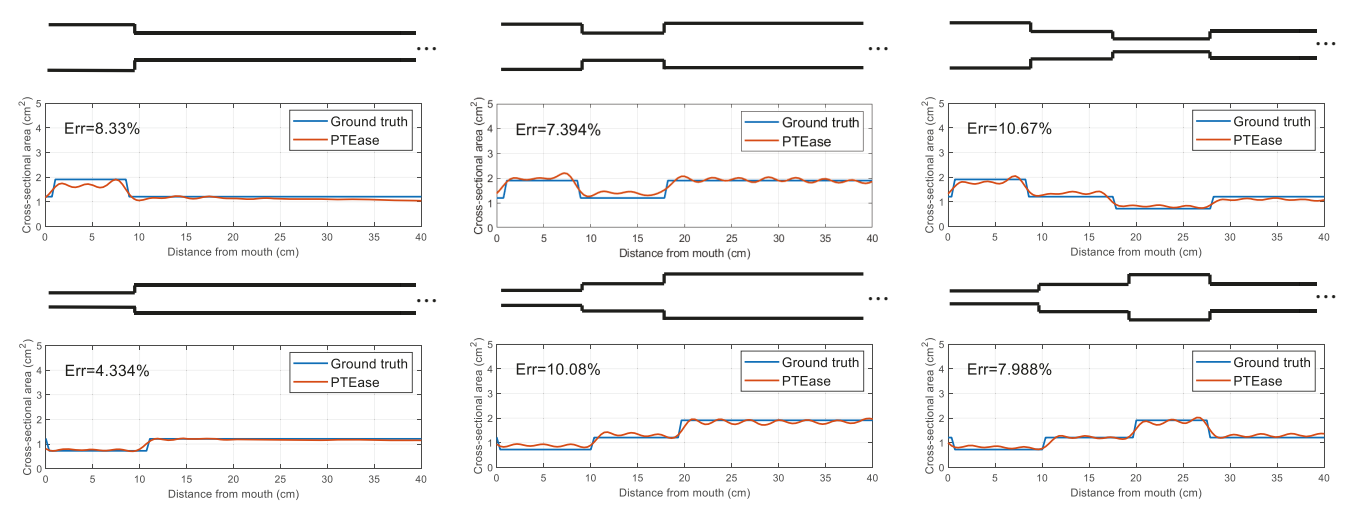


Figure 21: CSA measurements of concatenated plastic tubes

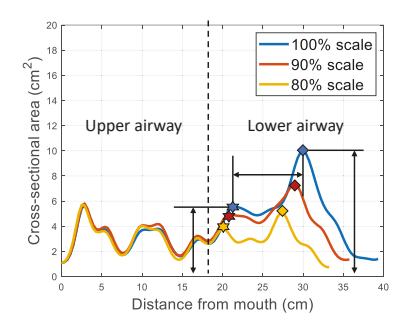


Figure 22: CSA measurements of airway models

Second, we evaluate the measurement accuracy of PTEase over 3D-printed human airway models, and evaluation results using a Samsung Galaxy S8 smartphone are in Figure 22. Since it is hard to measure the CSA at different airway segments as the ground truth, we instead evaluate the measurement accuracy at key airway structures. More specifically, we measure the amplitude of the two peaks in lower airway that represent the inlet of trachea and the carina, as well as the distance between these two peaks. As shown in Table 1, when compared with the measurement of 100% scale model, measurement results of 90% and 80% scale models precisely reflect the difference in 3D-printed scales, with an average error of 4.25 \pm 2.32%. Note that since airway models are printed in different scales of airway diameter, percentages in Table 1 are ratios of measured airway diameters at peak locations, as the square root of CSA.

Scale	Amplitude of	Amplitude of	Distance be-
(%)	first peak (cm ²)	second peak	tween two
		(cm^2)	peaks (cm)
100	5.565 (100%)	9.972 (100%)	8.58 (100%)
90	4.912 (93.95%)	7.373 (85.99%)	8.21 (87.63%)
80	3.803 (82.67%)	5.058 (71.22%)	7.51 (83.72%)

Table 1: Measurement of airway models

8.2 Human Subject Tests

We also tested PTEase on three healthy student volunteers in a lab-controlled environment and compared the measurement results to the reference airway CSA curve in Figure 12 to calculate each measurement's quality score. As shown in Figure 23, PTEase can

give relatively stable results on the same subject. From those measurements with scores higher than 80 and classified as "acceptable" by the NN classifier, we can easily identify the key airway structures from the CSA measurements. Note that not all human tests are able to generate acceptable airway measurement results with high quality. In Section 9, we will further evaluate the average quality score of airway measurements from a larger cohort of patients recruited in our clinical study.

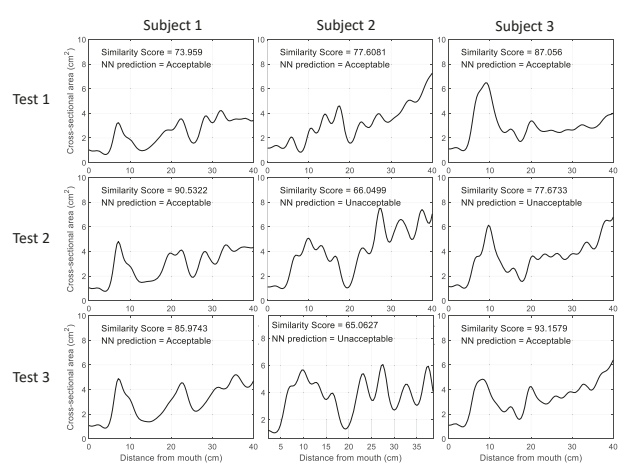


Figure 23: Airway measurements on human subjects

8.3 Measurement Accuracy on Different Smartphone Models

The frequency gains of microphone and speaker are heterogeneous on different smartphone models [53], resulting in different acoustic signals being transmitted and received. To investigate the impact of such smartphone hardware heterogeneity, we compare the airway measurement accuracy on two mainstream smartphone models, the Samsung Galaxy S8 and the Oneplus 7 Pro. Comparison results on concatenated plastic tubes are in Figure 24, which shows that the variation of measurement accuracy across these two smartphone models is within 1%. These results verified that PTEase can effectively tackle smartphone hardware heterogeneity.

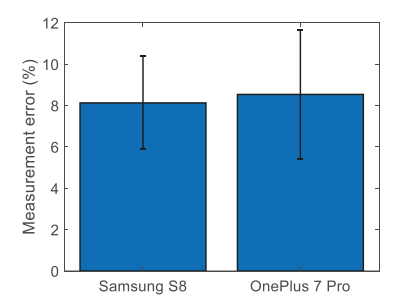


Figure 24: Accuracy with different smartphone models

8.4 The Impact of Signal's Frequency Bands

In practice, smartphone speakers and microphones usually have imbalanced gains in different frequency bands [53]. We investigate the impact of the transmitted signal's frequency bands on the measurement accuracy, by applying low-pass filters with different cut-off frequencies on the transmitted signal from a Samsung Galaxy S8 smartphone. Experiment results in Figure 25 show that using a higher cut-off frequency provides higher resolution in airway measurement, but may also increase the chance of measurement errors. Since the assumption of 1-D plane wave propagation generally holds within the frequency band <5.7 kHz as described in Section 3, we will use 6 kHz as the cut-off frequency in the rest of this paper.

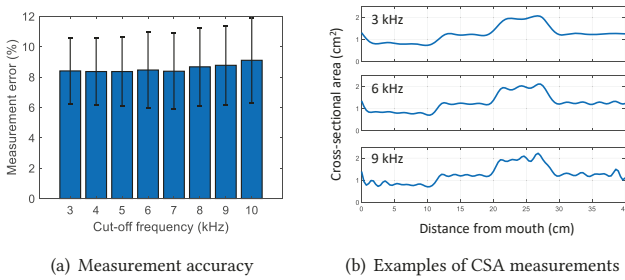


Figure 25: Impact of different frequency bands

8.5 The Impact of Ambient Noise

When being used in telemedicine settings, PTEase's airway measurement may be affected by various types of noises from the surrounding environment. In our evaluations, we tested PTEase's reliability against multiple types of ambient noises, including 1) a quiet office environment, 2) white noise from a working 3D printer, and 3) vocal sounds from another nearby smartphone playing videos at the highest volume. Averaged noise levels in these three scenarios are 31.2dB, 45.7dB, and 55.6dB, respectively, measured using the SoundMeter smartphone app⁴ on the same experiment device. Experiment results in Figure 26 show that PTEase can achieve reliable measurements in both cases. In particular, white noise has negligible impact on PTEase's airway measurement, and vocal sounds from video playback only incur 2% extra measurement errors. The major reason for such reliability is that PTEase transmits and receives the acoustic signal in a confined passage, which significantly attenuates the propagation of ambient noise.

8.6 Computing Latency and Energy Efficiency

From our experiment results, calculating airway CSA measurements from the received acoustic signal on smartphones can always be

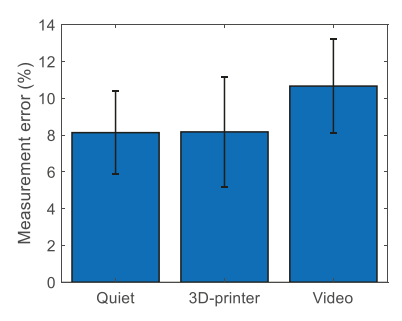


Figure 26: Measurement accuracy with ambient noise

completed within 10 seconds. After airway measurements have been uploaded to the server which takes 2 to 5 seconds depending on the wireless link condition, the ML model's inference time is always within 1 second. As a result, after the user completes an airway measurement, PTEase can provide results of lung function estimation and disease prediction within 15-30 seconds.

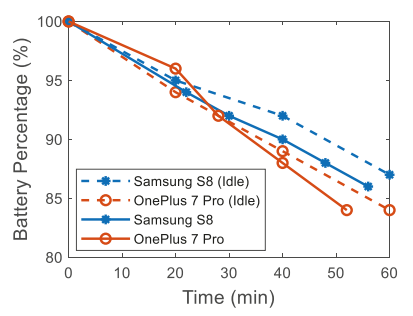


Figure 27: Power consumption of PTEase

We also evaluate PTEase's energy efficiency when it continuously transmits high-power acoustic signals for airway measurements. The results in Figure 27 show that, one hour of continuous PTEase usage consumes 15% to 20% of the smartphone's battery life, which is only 2% to 3% higher than the baseline power consumption (the smartphone stays idle and keeps screen on). However, since in practice each airway measurement in PTEase only lasts for a few seconds, PTEase's power consumption is as negligible in real use.

Category	Characteristics	Number
	Tests per subject	3.59 ± 0.87
	Age (years)	20.96 ± 15.21
Demographics	Adults (%)	69(37.91)
Demographics	Female (%)	92(50.55)
	Caucasian (%)	136(74.73)
	African-American (%)	47(25.82)
Body conditions	Height (cm)	159.35 ± 16.24
body collabolis	Weight (kg)	66.25 ± 26.92
	Healthy (%)	42(23.08)
Disease Condition	Asthma (%)	112(61.54)
	Cystic Fibrosis (%)	28(15.38)

Table 2: Human Subjects' Information

9 CLINICAL STUDY

Based on our accurate airway measurements in lab-controlled settings, we further conduct an observational clinical study to investigate the measurement accuracy of PTEase in patients with

 $^{^4} https://play.google.com/store/apps/details?id=com.ktwapps.soundmeter.\\$

Category	FEV1 Error (%)	FEV1/FVC Error (%)	Test-level Accuracy (%)	Subject-level Accuracy (%)
Healthy vs. Asthma	11.50 ± 0.57	15.19 ± 0.38	78.65 ± 2.8	77.78 ± 1.6
Healthy vs. CF	11.12 ± 0.83	15.17 ± 0.66	73.41 ± 4.51	71.32 ± 4.67
Average	11.31 ± 0.70	15.18 ± 0.52	76.03 ± 3.65	74.55 ± 3.14

Table 3: Accuracy of Lung Function Estimation and Disease Prediction

pulmonary diseases. With the IRB approval from the Children's Hospital of Pittsburgh, we recruit 182 human subjects in 12 months. As shown in Table 2, our subjects cover a wide variety of ages, genders, races, body conditions, and diseases. Each subject is instructed to select a mouthpiece of the proper size (100%/90%/75%/50%) and conduct several PTEase tests under the observation of clinicians. Detailed instructions were provided, including documentation, onscreen instructions, and demo videos. In each test, the subject is required to complete three respiratory cycles, and each inhalation/exhalation lasts for 5 seconds. The best exhalation measurement among the three respiratory cycles is then selected for further data analysis, and invalid data is removed using the method described in Sec 4.2.

Among the 182 human subjects, a total number of 495 airway measurements from 175 subjects are collected and considered valid, with an effectiveness of 96%. The average quality score of these measurements is 85. This high quality score indicates that PTEase's airway measurement system, including its calibration procedure and protocol of smartphone use, can be correctly operated by the study participants including children at low ages.

9.1 Accuracy of Pulmonary Disease Evaluation

Since our clinical study includes human subjects with different diseases (Asthma and CF), we target two separate classification tasks of disease prediction: 1) distinguish an asthma patient from healthy subjects, and 2) distinguish a CF patient from healthy subjects. For each task, we use 5-fold cross-validation to construct training and testing datasets from our collected clinical data, and use the physician's clinical diagnosis of disease condition, which are extracted from the patients' health records, as the ground truth labels. The estimation accuracy of FEV1 and FEV1/FVC is given in the form of percentage error, and the prediction accuracy is evaluated based on both levels of individual airway measurement tests and different subjects. The results are given in Table 3.

Overall, we can achieve an average accuracy of 74.55% for subject-level disease prediction, which is comparable to the prediction accuracy in clinical practice using spirometry data [26, 49]. The error for estimating the lung function indices, i.e., FEV1 and FEV1/FVC, is 11.31% and 15.18%, respectively. This accuracy is within the 10-18% error range of portable spirometry, which however, requires extra equipment, forced maneuvers, and professional coaching [44]. Therefore, PTEase can be sufficiently accurate to be used as an assistive tool for disease evaluation and monitoring.

In particular, the prediction accuracy of asthma is around 6% higher than that of CF. The reason for such difference is that the group of asthma patients is 4 times larger than the group of CF patients, which hence results in significantly higher learning difficulty. However, our results show that even with such a small amount of data, we can still achieve higher than 70% prediction accuracy.

We also evaluated the sensitivity and specificity of disease prediction in both classification tasks. The results in Table 4 show that

Category	Sensitivity (%)	Specificity (%)
Healthy vs. Asthma	82.54 ± 2.42	66.59 ± 5.49
Healthy vs. CF	68.20 ± 5.81	74.17 ± 7.78
Average	75.37 ± 4.12	70.33 ± 6.64

Table 4: Subject-level Sensitivity and Specificity of Disease Prediction

the sensitivity and specificity of asthma prediction are 82% and 66%, respectively. These results indicate that PTEase can be used as a useful screening tool to effectively identify most patients with potential asthma risks, hence suggesting further clinical tests for more affirmative disease diagnosis. On the other hand, the sensitivity and specificity of CF prediction are 68% and 74%, respectively. The main reason of such difference is that the number of CF patients in our clinical study is much smaller than that of asthma patients, and further involving more CF patients will be our next step to further evaluate PTEase's effectiveness in CF evaluation and prediction.

9.2 Accuracy over Different Patient Subgroups

In practice, patients' airway conditions and lung functions are highly correlated with age, gender, and the disease they have. Hence, we evaluate the accuracy of PTEase's disease evaluation in different patient subgroups of age, gender, and disease condition. Results of disease prediction and lung function estimation are shown in Figure 28 and 29, respectively.

First, in different age groups, we can see that PTEase achieves lower accuracy in disease prediction among children but higher accuracy in estimating their lung functions. A possible reason is that children's lung functions are highly correlated with their age and body size. Since PTEase measures the geometric dimensions of the airway which also has a strong correlation with age and height, it could help reduce the estimation errors of lung function indices. Second, in different gender groups, PTEase generally achieves better measurement accuracy on females compared to males, possibly because females are more willing to follow the PTEase app's instructions and provide better quality in airway measurements. Finally, in different disease groups, PTEase achieves the highest prediction accuracy among asthma patients, because of the imbalance between datasets of asthma and CF patients.

10 RELATED WORK

Mobile smart health. PTEase's sensing approach is related to the existing smartphone-based sensing systems. Typical spirometer-like approaches require expensive external sensing hardware that is attached to the smartphone via cable, WiFi, or Bluetooth [1, 57, 61], but PTEase does not require any of such extra sensing or computing hardware. Smartphones are also used to monitor heartbeat and respiratory intervals, by externally measuring chest motion [48]. Other acoustic sensing approaches use smartphone's built-in

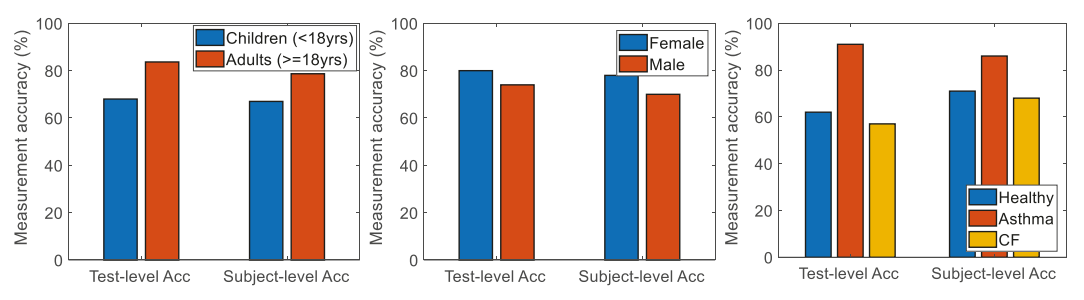


Figure 28: Accuracy of disease prediction over different patient subgroups

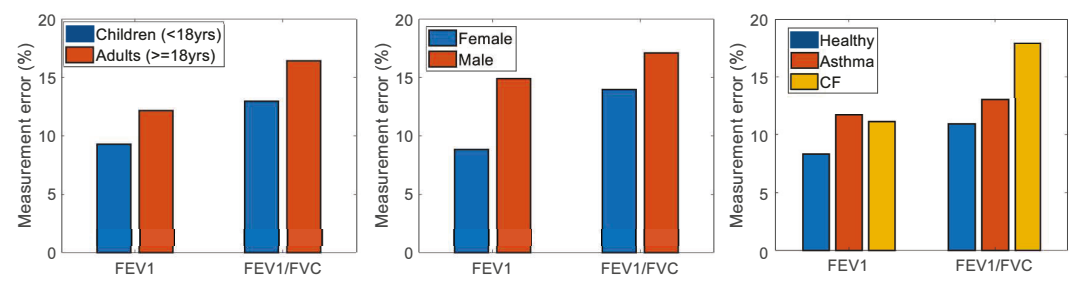


Figure 29: Accuracy of lung function estimation over different patient subgroups

microphones to passively overhear the breathing sounds and estimate the exhalation flow rate to give lung function predictions [21, 28, 62], but provide limited information about the airway's internal physiological conditions. In contrast, our sensing approach in PTEase provides direct information about the airway's internal conditions by measuring the airway CSA, and could hence better help clinical diagnosis in telemedicine settings.

AI-assisted disease diagnosis. PTEase's ML model builds on recent advances in using NNs for medical biomarker estimation and disease prediction. However, most of the existing work [10, 51, 54] assumes the availability of sufficient clinic data for training and hence directly uses off-the-shelf NN architectures. Instead, PTEase considers limited training data in practice and develops specialized ML models to ensure efficient NN training.

11 DISCUSSIONS & FUTURE WORK

Avoiding passage assembly. As shown in Section 4, errors in airway measurements are largely caused by the users' self-assembly of the passage and sensing system. One possibility of avoiding such assembly is to develop a new design of a one-piece disposable passage that replaces the current combination of smartphone adaptor, connecting tube, and mouthpiece, but a major challenge is to find the appropriate flexible materials for 3D printing.

Achieving better sensing accuracy. The accuracy of our current sensing approach is limited by the variability of CSA measurements, which is mainly caused by error accumulation in the WA algorithm: small system noise can lead to large variations in airway measurements. We could mitigate such impact of noise and error accumulation by inserting NN models into each iteration of CSA calculation, to predict and compensate the impact of accumulated noise. Such NN-assisted processing of acoustic signals will be our future work.

Predicting disease exacerbations. Patients with pulmonary disease can develop acute exacerbations with severe or fatal outcomes. The key to timely predicting such exacerbations is that the ML

model should be self-evolving to continuously acquire new knowledge about each subject's different disease states, and adaptively incorporate these new contexts to model training. We can leverage reinforced continual learning to build a personalized ML model for each subject and continually train each model with up-to-date airway measurements and disease condition records collected from the subject. Such personalized knowledge can help the model better monitor the progress of the disease.

Privacy of personal health data. Users may be concerned about the privacy of their personal data of airway conditions, if such data is being transmitted to a remote server for disease evaluation. In these cases, with the NN models being trained as described in Section 6, we can opt to implement PTEase to be a completely offline system, using an on-device ML framework (e.g., TensorFlow Lite) for model inference on smartphones without transmitting any data of airway measurements to a remote server. Updates of NN models, on the other hand, can be conducted via distributed learning methods such as federated learning [47, 58], to further avoid privacy leakage from users.

12 CONCLUSION

In this paper, we present PTEase, a new system design that transforms a commodity smartphone into a pulmonary telemedicine examination device that measures the internal physiological conditions of the human airway. We implemented PTEase as a smartphone app, and verified its measurement error in lab-controlled settings as <10%. Clinical studies further showed that PTEase can achieve 11% to 15% error in lung function estimation, and 75% accuracy in predicting pulmonary diseases.

ACKNOWLEDGMENTS

We thank the anonymous shepherd and reviewers for their comments and feedback. This work was supported in part by National Science Foundation (NSF) under grant number CNS-1812407, CNS-2029520, IIS-1956002, IIS-2205360, CCF-2217003 and CCF-2215042.

REFERENCES

- [1] 2022. MIR SmartOne. https://www.mirsmartone.com
- [2] Abbas K Abbas, Konrad Heimann, Katrin Jergus, Thorsten Orlikowsky, and Steffen Leonhardt. 2011. Neonatal non-contact respiratory monitoring based on real-time infrared thermography. Biomedical engineering online 10, 1 (2011), 1–17.
- [3] Katayoun Bahadori, Mary M Doyle-Waters, Carlo Marra, Larry Lynd, Kadria Alasaly, John Swiston, and Js Mark FitzGerald. 2009. Economic burden of asthma: a systematic review. BMC pulmonary medicine 9, 1 (2009), 1–16.
- [4] Peter J Barnes, Stanley J Szefler, Helen K Reddel, and Bradley E Chipps. 2019. Symptoms and perception of airway obstruction in asthmatic patients: clinical implications for use of reliever medications. *Journal of Allergy and Clinical Immunology* 144, 5 (2019), 1180–1186.
- [5] Louis M Bell, Robert Grundmeier, Russell Localio, Joseph Zorc, Alexander G Fiks, Xuemei Zhang, Tyra Bryant Stephens, Marguerite Swietlik, and James P Guevara. 2010. Electronic health record-based decision support to improve asthma care: a cluster-randomized trial. *Pediatrics* 125, 4 (2010), e770–e777.
- [6] Cristine E Berry, Meilan K Han, Bruce Thompson, Andrew H Limper, Fernando J Martinez, Marvin I Schwarz, Frank C Sciurba, Gerald J Criner, and Robert A Wise. 2015. Older adults with chronic lung disease report less limitation compared with younger adults with similar lung function impairment. Annals of the American Thoracic Society 12, 1 (2015), 21–26.
- [7] Eamann Breatnach, Gypsy C Abbott, and Robert G Fraser. 1984. Dimensions of the normal human trachea. American Journal of Roentgenology 142, 5 (1984), 903–906.
- [8] K Brown, C Aun, E Jackson, A Mackersie, D Hatch, and J Stocks. 1998. Validation of respiratory inductive plethysmography using the Qualitative Diagnostic Calibration method in anaesthetized infants. European Respiratory Journal 12, 4 (1998), 935–943.
- [9] David G Chapman, Cindy Thamrin, and Gregory G King. 2020. Perception of Symptoms as the Next Frontier for Personalized Medicine. The Journal of Allergy and Clinical Immunology: In Practice 8, 8 (2020), 2651–2652.
- [10] Zhe Chen, Tianyue Zheng, Chao Cai, and Jun Luo. 2021. MoVi-Fi: Motion-robust vital signs waveform recovery via deep interpreted RF sensing. In Proceedings of the 27th Annual International Conference on Mobile Computing and Networking. 392–405.
- [11] Kevin A Cook, Brian D Modena, and Ronald A Simon. 2016. Improvement in asthma control using a minimally burdensome and proactive smartphone application. The Journal of Allergy and Clinical Immunology: In Practice 4, 4 (2016), 730–737.
- [12] Robert O Crapo. 1994. Pulmonary-function testing. New England Journal of Medicine 331, 1 (1994), 25–30.
- [13] Koundinya Desiraju and Anurag Agrawal. 2016. Impulse oscillometry: the state-of-art for lung function testing. Lung India: official organ of Indian Chest Society 33, 4 (2016), 410.
- [14] Christopher M Evans, Kyubo Kim, Michael J Tuvim, and Burton F Dickey. 2009. Mucus hypersecretion in asthma: causes and effects. Current opinion in pulmonary medicine 15, 1 (2009), 4.
- [15] David A Fedele, J Graham Thomas, Andrew McConville, Elizabeth L McQuaid, Sara Voorhees, David M Janicke, Mutasim Abu-Hasan, Xiaofei Chi, and Matthew J Gurka. 2021. Using mobile Health to improve asthma self-Management in early Adolescence: a pilot randomized controlled trial. *Journal of Adolescent Health* 69, 6 (2021), 1032–1040.
- [16] Emma Fettes, Mollie Riley, Stephanie Brotherston, Claire Doughty, Benjamin Griffiths, Aidan Laverty, and Paul Aurora. 2022. "You're on mute!" Does pediatric CF home spirometry require physiologist supervision? *Pediatric Pulmonology* 57, 1 (2022), 278–284.
- [17] James E Fish and Stephen P Peters. 1999. Airway remodeling and persistent airway obstruction in asthma. Journal of Allergy and Clinical Immunology 104, 3 (1999), 509–516.
- [18] Erick Forno, Neethu Abraham, Daniel G Winger, Christian Rosas-Salazar, Geoffrey Kurland, and Daniel J Weiner. 2018. Perception of pulmonary function in children with asthma and cystic fibrosis. *Pediatric allergy, immunology, and pulmonology* 31, 3 (2018), 139–145.
- [19] Jeffrey J Fredberg. 1981. Acoustic determinants of respiratory system properties. Annals of biomedical engineering 9, 5 (1981), 463–473.
- [20] Frederick LGR Gerzon, Quirijn Jöbsis, Michiel AGE Bannier, Bjorn Winkens, and Edward Dompeling. 2020. Discrepancy between lung function measurements at home and in the hospital in children with asthma and CF. Journal of Clinical Medicine 9, 6 (2020), 1617.
- [21] Mayank Goel, Elliot Saba, Maia Stiber, Eric Whitmire, Josh Fromm, Eric C Larson, Gaetano Borriello, and Shwetak N Patel. 2016. Spirocall: Measuring lung function over a phone call. In Proceedings of the 2016 CHI conference on human factors in computing systems. 5675–5685.
- [22] Timothy H Harries and Patrick White. 2021. Spotlight on primary care management of COPD: electronic health records. , 1479973120985594 pages.
- [23] V Hoffstein and JJ Fredberg. 1991. The acoustic reflection technique for non-invasive assessment of upper airway area. European Respiratory Journal 4, 5 (1991), 602–611.

- [24] Mark Holt, Ben Yule, Dylan Jackson, Mary Zhu, and Neema Moraveji. 2018. Ambulatory monitoring of respiratory effort using a clothing-adhered biosensor. In 2018 IEEE International Symposium on Medical Measurements and Applications (MeMeA). IEEE, 1–6.
- [25] Chen-Yu Hsu, Aayush Ahuja, Shichao Yue, Rumen Hristov, Zachary Kabelac, and Dina Katabi. 2017. Zero-effort in-home sleep and insomnia monitoring using radio signals. Proceedings of the ACM on Interactive, mobile, wearable and ubiquitous technologies 1, 3 (2017), 1–18.
- [26] Kana Ram Jat. 2013. Spirometry in children. Primary Care Respiratory Journal 22, 2 (2013), 221–229.
- [27] Ibrahim Kamal. 2001. Normal standard curve for acoustic pharyngometry. Otolaryngology-Head and Neck Surgery 124, 3 (2001), 323–330.
- [28] Eric C Larson, Mayank Goel, Gaetano Boriello, Sonya Heltshe, Margaret Rosen-feld, and Shwetak N Patel. 2012. SpiroSmart: using a microphone to measure lung function on a mobile phone. In Proceedings of the 2012 ACM Conference on ubiquitous computing. 280–289.
- [29] Gregory F Lewis, Rodolfo G Gatto, and Stephen W Porges. 2011. A novel method for extracting respiration rate and relative tidal volume from infrared thermography. Psychophysiology 48, 7 (2011), 877–887.
- [30] Jian Liu, Yan Wang, Yingying Chen, Jie Yang, Xu Chen, and Jerry Cheng. 2015. Tracking vital signs during sleep leveraging off-the-shelf wifi. In Proceedings of the 16th ACM international symposium on mobile ad hoc networking and computing. 267–276.
- [31] Mario Morais-Almeida, Miguel Barbosa, and Claudia Sousa. 2022. Telemedicine in the Management of Chronic Obstructive Respiratory Diseases: An Overview. Exon Publications (2022), 131–144.
- [32] Meinard Müller. 2007. Dynamic time warping. Information retrieval for music and motion (2007), 69–84.
- [33] Sherry L Murphy, Kenneth D Kochanek, Jiaquan Xu, and Elizabeth Arias. 2021. Mortality in the United States. NCHS data brief No. 427 (2021).
- [34] Yunyoung Nam, Youngsun Kong, Bersain Reyes, Natasa Reljin, and Ki H Chon. 2016. Monitoring of heart and breathing rates using dual cameras on a smartphone. PloS one 11, 3 (2016), e0151013.
- [35] Rajalakshmi Nandakumar, Shyamnath Gollakota, and Jacob E Sunshine. 2019. Opioid overdose detection using smartphones. Science translational medicine 11, 474 (2019), eaau8914.
- [36] Rajalakshmi Nandakumar, Shyamnath Gollakota, and Nathaniel Watson. 2015. Contactless sleep apnea detection on smartphones. In Proceedings of the 13th annual international conference on mobile systems, applications, and services. 45– 57.
- [37] Phuc Nguyen, Xinyu Zhang, Ann Halbower, and Tam Vu. 2016. Continuous and fine-grained breathing volume monitoring from afar using wireless signals. In IEEE INFOCOM 2016-The 35th Annual IEEE International Conference on Computer Communications. IEEE, 1–9.
- [38] Imre Noth, Vincent Cottin, Nazia Chaudhuri, Tamera J Corte, Kerri A Johannson, Marlies Wijsenbeek, Stephane Jouneau, Andreas Michael, Manuel Quaresma, Klaus B Rohr, et al. 2021. Home spirometry in patients with idiopathic pulmonary fibrosis: data from the INMARK trial. European Respiratory Journal 58, 1 (2021).
- [39] Sean B O'Loghlen, Linda Levesque, Thomas Fisher, Yvonne DeWit, Marlo White-head, Teresa To, and M Diane Lougheed. 2020. Health services utilization is increased in poor perceivers of bronchoconstriction and hyperinflation in asthma. The Journal of Allergy and Clinical Immunology: In Practice 8, 8 (2020), 2643–2650.
- [40] Ellie Oostveen, D MacLeod, H Lorino, R Farre, Z Hantos, K Desager, F Marchal, et al. 2003. The forced oscillation technique in clinical practice: methodology, recommendations and future developments. European respiratory journal 22, 6 (2003), 1026–1041.
- [41] Alex Paynter, Umer Khan, Sonya L Heltshe, Christopher H Goss, Noah Lechtzin, and Nicole Mayer Hamblett. 2022. A comparison of clinic and home spirometry as longtudinal outcomes in cystic fibrosis. *Journal of Cystic Fibrosis* 21, 1 (2022), 78–83.
- [42] Philip H Quanjer, Sanja Stanojevic, Tim J Cole, Xaver Baur, Graham L Hall, Bruce H Culver, Paul L Enright, John L Hankinson, Mary SM Ip, Jinping Zheng, et al. 2012. Multi-ethnic reference values for spirometry for the 3–95-yr age range: the global lung function 2012 equations.
- [43] Tauhidur Rahman, Alexander T Adams, Mi Zhang, Erin Cherry, Bobby Zhou, Huaishu Peng, and Tanzeem Choudhury. 2014. Bodybeat: A mobile system for sensing non-speech body sounds. In Proceedings of the 12th annual international conference on Mobile systems, applications, and services. 2–13.
- [44] Rachelle R Ramsey, Jill M Plevinsky, Lauren Milgrim, Kevin A Hommel, Karen M McDowell, Jeffrey Shepard, and Theresa W Guilbert. 2021. Feasibility and preliminary validity of mobile spirometry in pediatric asthma. The Journal of Allergy and Clinical Immunology: In Practice 9, 10 (2021), 3821–3823.
- [45] Helen K Reddel, Leonard B Bacharier, Eric D Bateman, Christopher E Brightling, Guy G Brusselle, Roland Buhl, Alvaro A Cruz, Liesbeth Duijts, Jeffrey M Drazen, J Mark FitzGerald, et al. 2022. Global Initiative for Asthma Strategy 2021: executive summary and rationale for key changes. American Journal of Respiratory and Critical Care Medicine 205, 1 (2022), 17–35.

- [46] MICHAEL D Revow, SANDRA J England, HA Stogryn, and DONNA L Wilkes. 1987. Comparison of calibration methods for respiratory inductive plethysmography in infants. *Journal of Applied Physiology* 63, 5 (1987), 1853–1861.
- [47] Nicola Rieke, Jonny Hancox, Wenqi Li, Fausto Milletari, Holger R Roth, Shadi Albarqouni, Spyridon Bakas, Mathieu N Galtier, Bennett A Landman, Klaus Maier-Hein, et al. 2020. The future of digital health with federated learning. NPJ digital medicine 3, 1 (2020), 119.
- [48] M Scarpetta, M Spadavecchia, G Andria, MA Ragolia, and N Giaquinto. 2022. Accurate simultaneous measurement of heartbeat and respiratory intervals using a smartphone. *Journal of Instrumentation* 17, 07 (2022), P07020.
- [49] Antonius Schneider, Lena Gindner, Lisa Tilemann, Tjard Schermer, Geert-Jan Dinant, Franz Joachim Meyer, and Joachim Szecsenyi. 2009. Diagnostic accuracy of spirometry in primary care. BMC pulmonary medicine 9, 1 (2009), 1–10.
- [50] Amirhossein Shahshahani, Carl Laverdiere, Sharmistha Bhadra, and Zeljko Zilic. 2018. Ultrasound sensors for diaphragm motion tracking: An application in non-invasive respiratory monitoring. Sensors 18, 8 (2018), 2617.
- [51] Xingzhe Song, Boyuan Yang, Ge Yang, Ruirong Chen, Erick Forno, Wei Chen, and Wei Gao. 2020. SpiroSonic: monitoring human lung function via acoustic sensing on commodity smartphones. In Proceedings of the 26th Annual International Conference on Mobile Computing and Networking. 1–14.
- [52] R Thurnheer. 1999. Pharyngeal cross-sectional area and compliance in normal males and females. Respiration; international review of thoracic diseases 66, 4 (1999), 382.
- [53] Yu-Chih Tung, Duc Bui, and Kang G Shin. 2018. Cross-platform support for rapid development of mobile acoustic sensing applications. In Proceedings of the 16th Annual International Conference on Mobile Systems, Applications, and Services. 455–467.
- [54] Shuai Wang, Bo Kang, Jinlu Ma, Xianjun Zeng, Mingming Xiao, Jia Guo, Mengjiao Cai, Jingyi Yang, Yaodong Li, Xiangfei Meng, et al. 2021. A deep learning algorithm

- using CT images to screen for Corona Virus Disease (COVID-19). European radiology 31, 8 (2021), 6096–6104.
- [55] Jerry A Ware and Kehti Aki. 1969. Continuous and discrete inverse-scattering problems in a stratified elastic medium. I. Plane waves at normal incidence. The journal of the Acoustical Society of America 45, 4 (1969), 911–921.
- [56] DE Weston. 1953. The theory of the propagation of plane sound waves in tubes. *Proceedings of the Physical Society. Section B* 66, 8 (1953), 695.
 [57] Marlies S Wijsenbeek, Catharina C Moor, Kerri A Johannson, Peter D Jackson,
- [57] Marlies S Wijsenbeek, Catharina C Moor, Kerri A Johannson, Peter D Jackson, Yet H Khor, Yasuhiro Kondoh, Sujeet K Rajan, Gabriela C Tabaj, Brenda E Varela, Pieter van der Wal, et al. 2022. Home monitoring in interstitial lung diseases. The Lancet Respiratory Medicine (2022).
- [58] Qiang Yang, Yang Liu, Tianjian Chen, and Yongxin Tong. 2019. Federated machine learning: Concept and applications. ACM Transactions on Intelligent Systems and Technology (TIST) 10, 2 (2019), 1–19.
- [59] Meng-Chieh Yu, Jia-Ling Liou, Shuenn-Wen Kuo, Ming-Sui Lee, and Yi-Ping Hung. 2012. Noncontact respiratory measurement of volume change using depth camera. In 2012 Annual International Conference of the IEEE Engineering in Medicine and Biology Society. IEEE, 2371–2374.
- [60] Shichao Yue, Hao He, Hao Wang, Hariharan Rahul, and Dina Katabi. 2018. Extracting multi-person respiration from entangled RF signals. Proceedings of the ACM on Interactive, Mobile, Wearable and Ubiquitous Technologies 2, 2 (2018), 1–22.
- [61] Ping Zhou, Liu Yang, and Yao-Xiong Huang. 2019. A smart phone based handheld wireless spirometer with functions and precision comparable to laboratory spirometers. Sensors 19, 11 (2019), 2487.
- [62] Fatma Zubaydi, Assim Sagahyroon, Fadi Aloul, Hasan Mir, and Bassam Mahboub. 2020. Using Mobiles to Monitor Respiratory Diseases. In *Informatics*, Vol. 7. MDPI, 56.